Mon. Not. R. Astron. Soc. **000**, 1–10 (2010) Printed 20 May 2011 (MN LATEX style file v2.2)

Autocorrelations of stellar light and mass at $z \sim 0$ and ~ 1: From SDSS to DEEP2

Cheng Li[1,2⋆],Simon D. M. White[2], Yanmei Chen[3],Alison L. Coil[4]†, Marc Davis[5], Gabriella De Lucia[6],Qi Guo[7],Y. P. Jing[1],Guinevere Kauffmann[2], Christopher N. A. Willmer[8] and Wei Zhang[9]

[1] *Partner Group of the MPI für Astrophysik at Shanghai Astronomical Observatory, Key Laboratory for Research in Galaxies and Cosmology of Chinese Academy of Sciences, Nandan Road 80, Shanghai 200030, China*
[2] *Max-Planck-Institute für Astrophysik, Karl-Schwarzschild-Str. 1, D-85741 Garching, Germany*
[3] *Department of Astronomy, Nanjing University, Nanjing 210093, China*
Key Laboratory of Modern Astronomy and Astrophysics (Nanjing University), Ministry of Education, Nanjing 210093, China
[4] *Department of Physics, Center for Astrophysics and Space Sciences, University of California, 9500 Gilman Dr., La Jolla, San Diego, CA 92093, USA*
[5] *Department of Astronomy, University of California, Berkeley, CA 94720, USA*
[6] *INAF - Astronomical Observatory of Trieste, via G.B. Tiepolo 11, I-34143 Trieste, Italy*
[7] *Institute for Computational Cosmology, Department of Physics, University of Durham, South Road, Durham, DH1 3LE, UK*
[8] *Steward Observatory, University of Arizona, Tucson, AZ 85721, USA*
[9] *National Astronomical Observatories, Chinese Academy of Sciences, Beijing 100012, China*

Accepted ..... Received .....; in original form .....

ABSTRACT

We present measurements of projected autocorrelation functions $w_p(r_p)$ for the stellar mass of galaxies and for their light in the U, B and V bands, using data from the third data release of the DEEP2 Galaxy Redshift Survey and the final data release of the Sloan Digital Sky Survey (SDSS). We investigate the clustering bias of stellar mass and light by comparing these to projected autocorrelations of dark matter estimated from the Millennium Simulations (MS) at $z = 1$ and 0.07, the median redshifts of our galaxy samples. All of the autocorrelation and bias functions show systematic trends with spatial scale and waveband which are impressively similar at the two redshifts. This shows that the well-established environmental dependence of stellar populations in the local Universe is already in place at $z = 1$. The recent MS-based galaxy formation simulation of Guo et al. (2011) reproduces the scale-dependent clustering of luminosity to an accuracy better than 30% in all bands and at both redshifts, but substantially overpredicts mass autocorrelations at separations below about 2 Mpc. Further comparison of the *shapes* of our stellar mass bias functions with those predicted by the model suggests that both the SDSS and DEEP2 data prefer a fluctuation amplitude of $\sigma_8 \sim 0.8$ rather than the $\sigma_8 = 0.9$ assumed by the MS.

Key words: galaxies: clusters: general – galaxies: distances and redshifts – cosmology: theory – dark matter – large-scale structure of Universe.

1 INTRODUCTION

The two-point correlation function (2PCF) has long served as the primary way of quantifying the spatial distribution of galaxies in our Universe. Measurements of 2PCF for different classes of galaxies in the local Universe have been carried out with high accuracy thanks to the large redshift surveys assembled in recent years, in particular the two-degree field galaxy redshift survey (2dFGRS; Colless et al. 2001) and the Sloan Digital Sky Survey (SDSS; York et al. 2000). These studies have established that 2PCFs depend on a variety of properties such as luminosity, stellar mass, colour, spectral type and morphology (Davis et al. 1988; Hamilton 1988; White et al. 1988; Boerner et al. 1989; Einasto 1991; Park et al. 1994; Loveday et al. 1995; Benoist et al. 1996; Guzzo et al. 1997; Willmer et al. 1998; Loveday et al. 1999; Beisbart & Kerscher 2000; Brown et al. 2000; Guzzo et al. 2000; Norberg et al. 2001, 2002; Zehavi et al. 2002, 2005; Li et al. 2006b; Wang et al. 2007; Swanson et al. 2008;

⋆ E-mail: leech@shao.ac.cn
† Alfred P. Sloan Foundation Fellow

Zehavi et al. 2010; Wang et al. 2010; Ross et al. 2011). Recently, there have also been studies of galaxy clustering at higher redshifts, which are usually based on deep surveys (up to $z \sim 1-1.5$) covering small areas ($\lesssim$1.5 deg^2), e.g. the DEEP2 Galaxy Redshift Survey (Davis et al. 2003; Coil et al. 2004a, 2006, 2008), the VIMOS-VLT Deep Survey (Le Fèvre et al. 2005; Pollo et al. 2005, 2006; Meneux et al. 2006, 2008), and the zCOSMOS Survey (Lilly et al. 2007, 2009; Meneux et al. 2009; de la Torre et al. 2011a). Measurements of 2PCFs for different classes of galaxies and at different redshifts have provided powerful quantitative constraints on models of galaxy formation and evolution (see for example De Lucia & Blaizot 2007; Li et al. 2007; Guo et al. 2011; de la Torre et al. 2011b).

A number of recent studies have further investigated the dependence of galaxy clustering on physical properties by measuring *weighted* or *marked* 2PCFs (e.g. Beisbart & Kerscher 2000; Faltenbacher et al. 2002; Sheth 2005; Skibba et al. 2006; Skibba & Sheth 2009; Skibba et al. 2009; Li & White 2009, 2010). Simply speaking, this statistic is estimated using exactly the same methodology as the one used for the traditional 2PCF, except that each galaxy in the real sample and/or in the random sample is weighted by one of its physical properties such as stellar mass or luminosity at a given band. When compared to the traditional 2PCF, this alternative two-point statistic has the advantage that it makes use of the whole galaxy sample and thus minimizes the sampling and large-scale structure noises. As found in Li & White (2009), a particular virtue of the weighted correlation functions is that the correlation signals are dominated by contributions from galaxies in a relatively narrow mass range, around the characteristic mass of the stellar mass function. Thus, the statistic is robust to incompleteness of the observed sample at the two mass extremes. In addition, the weighting scheme used for estimating the statistic makes it a direct measure of the clustering of *stars* on scales larger than those of individual galaxies, rather than the clustering of the host galaxies as probed by the traditional 2PCF. This statistic thus provides a compact and accurate way to characterize the distribution of stellar populations over large ranges in spatial scale.

Using a sample of almost half a million galaxies from the Sloan Digital Sky Survey (SDSS), Li & White (2009, hereafter Paper I) and Li & White (2010, hereafter Paper II) estimated projected autocorrelation functions $w_p(r_p)$ both for the stellar mass of galaxies and for their light in the five SDSS photometric bands. All of the autocorrelation estimates are extremely well described by power laws over the full non-linear range $10h^{-1}$kpc$< r_p < 10h^{-1}$Mpc. Luminosity is found to cluster less strongly than stellar mass in all bands and on all scales. The autocorrelation function of luminosity varies systematically with wavelength in both amplitude and slope, with the reddest band (the z band) showing the highest amplitude and the steepest slope, indicating that the z-band light is the closest proxy for stellar mass in terms of clustering properties. These trends provide a precise characterization of the well-known dependence of stellar populations on environment. In combination with autocorrelation functions of luminosity- and stellar mass-selected galaxy samples, as well as accurate luminosity and stellar mass functions, these results provide tight constraints on galaxy formation, which are a major challenge for current models (see, for example, the significant discrepancies in recent work by Guo et al. 2011 based on the Millennium Simulations).

In this paper, we extend the work of Papers I and II to higher redshifts ($z \sim 1$) using data from the DEEP2 Galaxy Redshift Survey (Davis et al. 2003). We use the methodology of Papers I and II to compute projected stellar mass autocorrelation functions for DEEP2 galaxies, as well as projected autocorrelations for their luminosity in the rest-frame U and B bands. In order to compare the two surveys directly, we re-analysize the SDSS, computing luminosity autocorrelations in the U, B and V bands, where luminosities in these bands are estimated from SDSS data through a Bayesian technique based on a spectral energy distribution library constructed from the Bruzual & Charlot (2003, hereafter BC03) population synthesis code. We compare these results with the autocorrelations of dark matter at $z = 0.07$ and $z = 1$, the median redshifts of the SDSS and DEEP2 galaxy samples used here, in order to understand the *bias* of stellar mass and light. By comparing with the model of Guo et al. (2011), we investigate quantitatively how well current treatments of galaxy formation reproduce the clustering evolution of stellar mass and light. Finally, we discuss the possibility that the measured shape of the mass autocorrelation functions can be used to estimate the value of the mass fluctuation amplitude parameter σ_8.

2 DATA

2.1 SDSS galaxy sample

The low-redshift galaxy sample used in this study is a magnitude-limited sample constructed from the final data release (DR7; Abazajian et al. 2009) of the SDSS (York et al. 2000) and is exactly the same as that used in Papers I and II. This sample contains 482,755 galaxies located in the main contiguous area of the survey in the northern Galactic cap, with $r < 17.6$, $-24 < M_{0.1r} < -16$ and spectroscopically measured redshifts in the range $0.001 < z < 0.5$. Here r is the r-band Petrosian apparent magnitude, corrected for Galactic extinction, and $M_{0.1r}$ is the r-band Petrosian absolute magnitude, corrected for evolution and K-corrected to its value at $z = 0.1$. The apparent magnitude limit is chosen in order to select a sample that is uniform and complete over the entire area of the survey (see Tegmark et al. 2004). The median redshift of this sample is $z = 0.088$, with 10% of the galaxies below z=0.033 and 10% above z=0.16. As shown in Paper I (see their fig. 4) the autocorrelation of stellar mass is dominated by contributions from a narrower and slightly lower redshift range (with 10% of the galaxies below $z = 0.025$ and 10% above $z = 0.12$), with a median redshift of $z = 0.067$. We thus take $z = 0.067$ as the *effective* median redshift of this sample when comparing with dark matter autocorrelations and semi-analytical model predictions.

We use a Bayesian technique to derive estimates of the absolute magnitudes in U, B and V bands for each galaxy in our sample, following Kauffmann et al. (2003) and Salim et al. (2005). Libraries of Monte Carlo realizations of model star formation histories are generated between $0 < z < 0.5$ in regular bins of $\Delta z = 0.001$, using

the BC03 population synthesis code. Each library contains 25000 models with each star formation history being characterized with two components: an underlying continuous model with an exponentially declining star formation law and random bursts superimposed on this continuous model. The models also have metallicities and dust attenuation uniformly distributed over wide ranges. The universal initial mass function (IMF) of Kroupa (2001) is adopted. For each galaxy in our sample, we derive the U, B and V magnitudes by comparing the observed *ugriz* SED to all the model SEDs in the closest redshift model library. The χ^2 goodness of fit of each model determines the weight, $\propto \exp(-\chi^2/2)$, which is assigned to that model when building the probability distribution functions (PDFs) of the restframe U, B and V magnitudes of the galaxy. We adopt the PDF-weighted *mean* values as our estimates of these quantities. Adopting the *median* of the PDF gives almost identical results for the autocorrelation function analysis.

2.2 DEEP2 galaxy sample

The DEEP2 Galaxy Redshift Survey (Davis et al. 2003) utilizes the DEIMOS spectrograph (Faber et al. 2003) on the KECK II telescope. Targets for the spectroscopic sample were selected from BRI photometry (Coil et al. 2004a) taken with the 12k x 8k mosaic camera on the Canada-France-Hawaii Telescope (CFHT). The images have a limiting magnitude of $R_{\rm AB} \sim 25.5$. Since the R-band provides the highest signal-to-noise ratio (S/N) among all the CFHT bands, the photometry in this band was used to select targets for spectroscopic observation in the DEEP2. The CFHT imaging covers four widely-separated regions, with a total area of 3.5 deg^2. In fields 2 to 4, the spectroscopic sample is preselected using $(B-R)$ and $(R-I)$ colors to eliminate objects with $z < 0.7$ (Davis et al. 2003). Color and apparent magnitude cuts were also applied to objects in the first field, the Extended Groth Strip (EGS), but these were designed to downweight low redshift galaxies rather than eliminate them entirely (Willmer et al. 2006).

We use data from the third data release of the DEEP2 survey[1] which contains spectra of about 50000 galaxies in the magnitude range $18.5 \leqslant R_{\rm AB} \leqslant 24.1$. The spectra have a resolution of $R \sim 5000$. For this study we have selected a sample of 30546 galaxies from the DEEP2 DR3, with redshifts of quality 3 or 4 and in the range $0.8 < z < 1.35$. The median redshift of this sample is $z = 1$, which we use for comparisons with dark matter and model galaxy autocorrelations.

The derived galaxy parameters required in this work include stellar mass (M_*) and restframe magnitudes in U and B bands. The procedure for estimating these parameters is exactly the same as the one above for the SDSS. In brief, the observed BRI SED of each galaxy in the DEEP2 is compared to a large grid of BC03 model SEDs, providing a maximum likelihood estimate of the I-band mass-to-light ratio of the galaxy, as well as its restframe U and B magnitudes. A Kroupa (2001) initial mass function (IMF) is adopted, as in the SDSS analysis. Our estimates of stellar mass and restframe magnitudes are statistically well consistent with those from Bundy et al. (2006) and Willmer et al. (2006). Indeed we have repeated our clustering analysis using stellar mass and restframe magnitude estimates from these previous papers, obtaining almost the same results.

We don't consider the V band for DEEP2 galaxies, as at $z \sim 1$ this band is shifted well beyond the reddest band (the I band) that is observed.

2.3 Semi-analytic model galaxy catalogues

In this paper we compare our observational results to predictions from the galaxy formation model of Guo et al. (2011, hereafter G11). This model was created by implementing semi-analytic models for baryonic astrophysics on merger trees encapsulating the evolution of the halo/subhalo population in the Millennium (Springel 2005) and Millennium-II (Boylan-Kolchin et al. 2009) Simulations[2]. The Millennium was carried out in a cubic region 500 h^{-1}Mpc on a side with mass resolution $\sim 10^9$ M$_\odot$, while the Millennium-II followed evolution in a region with 125 times smaller volume, but at 125 times better mass resolution. The combination of the two simulations allows galaxy formation to be studied over the full range of observed populations, from dwarf spheroidals to cD galaxies. In comparison to earlier semi-analytic models from the Munich group, the treatments of supernova feedback, galaxy size, photoionisation suppression and environmental effects on satellite galaxies have been significantly updated, resulting in excellent fits not only to recent SDSS data on the luminosity and stellar mass functions of galaxies, but also to the recent determinations of the abundance of faint satellite galaxies around the Milky-Way. Most of the population properties for galaxies in the local Universe are reasonably well reproduced by the model, which also makes precise predictions for nonlinear clustering over the full observed range of scales, 10 kpc to 10 Mpc. Comparisons between the clustering properties predicted by the model and measurements of SDSS galaxy clustering show that agreement with SDSS data is quite good for masses above $6 \times 10^{10} M_\odot$ and at separations above 2 Mpc, although the predicted clustering is up to 20% too high in some mass ranges. On smaller scales lower mass galaxies are predicted to be substantially more clustered than is observed. G11 suggest, but do not prove, that this may be a consequence of an overly large present-day fluctuation amplitude ($\sigma_8 = 0.9$) in the simulations.

3 CLUSTERING MEASURES

Following Papers I and II, we weight each galaxy in our samples to correct for incompleteness when computing our stellar mass (or luminosity) autocorrelations. The weights used for SDSS galaxies take into account three factors. The first is $1/f_{sp}$, where f_{sp} is a spectroscopic completeness, defined as the fraction of the photometrically defined target galaxies for which usable spectra were obtained. The second weight, $1/V_{ij}$, is applied to each pair of galaxies, where

[1] http://deep.berkeley.edu/DR3/

[2] Galaxy catalogues for this model and halo catalogues for the parent simulations are publicly available at http://www.mpa-garching.mpg.de/millennium

$V_{ij} = \min(V_{max,i}, V_{max,j})$ and $V_{max,i}$ is the maximum volume over which the ith galaxy would be included in the sample. This weight accounts for the fact that faint galaxies are not detected throughout the entire survey volume in a flux-limited survey. The final weight is the factor $1/f_{coll,ij}$, which is also applied to galaxy pairs and appears in data-data counts only. This factor is a function of angular separation θ_{ij} of the two galaxies and corrects for the effect of fibre collisions on small scales.

Similarly, for each galaxy pair in the DEEP2 sample we also assign a weight following Willmer et al. (2006):

$$W_{ij} = \frac{\kappa_i \kappa_j}{V_{ij}}, \quad (1)$$

where κ_i accounts for incompleteness resulting from the DEEP2 colour selection and redshift success rate. The second factor V_{ij} is defined in the same way as above. Detailed description on the calculation of the weights can be found in Willmer et al. (2006).

We have generated a random sample which has the same overall sky coverage and redshift distribution as the DEEP2 sample. The spatial window function of the DEEP2 survey is applied to the random sample, which includes masking areas around bright stars and takes into account the varying redshift completeness of the observed slit masks. The reader is referred to previous papers by Coil et al. (2004b, 2006, 2008) for detailed description of the window function. For each real galaxy we generate 100 sky positions at random within the entire survey region of the DEEP2 including all the four separate fields, and we assign to each of them the properties of the real galaxy, in particular, its values of κ and V_{max}. Since the four fields of the survey are widely separated, correlations in these properties in the real sample are wiped out by randomizing in angle. We follow Coil et al. (2006) to assign a redshift to each random point according to the redshift distribution averaged over all the fields in the data.

The projected autocorrelation function of stellar mass or luminosity in a given band is then computed using the estimator described in Paper I (see their eqn. 2), in which the weights obtained above are applied. We estimate the autocorrelation functions using the entire real (or random) sample, for both SDSS and DEEP2. Errors on the mass autocorrelation in the SDSS are estimated from the scatter among the measurements from 20 mock galaxy catalogues constructed from the Millennium Simulation using the same selection criteria as the real sample (see Paper I for details). The errors on the DEEP2 mass autocorrelation function come from the scatter among the measurements for the four separate fields of the survey. These errors should include both the effect of counting noise and that of *cosmic variance*, which are impressively small in the SDSS due to the large size and volume of the sample. Following Paper I, we do not attempt to put independent error bars on the projected luminosity autocorrelations because, for a given survey, with our technique the set of galaxy pairs used to estimate each of these functions is *exactly* the same and as a result the noise fluctuations due to sampling and to large-scale structure are identical in all autocorrelation estimates.

It is important to point out that we have ignored the undersampling of DEEP2 galaxies on small scales due to the slit mask target-selection algorithm. Coil et al. (2006) use the mock galaxy catalogue of Yan et al. (2004) to correct for the effect of this on their measurements of projected two-point autocorrelation functions, finding that the corrections are most significant on scales less than $r_p = 0.3h^{-1}$Mpc. This scale is close to the lower limit ($r_p \sim 0.2h^{-1}$Mpc) to which we plot our autocorrelation functions. We decided not to attempt to correct for slit mask effects, but one should keep in mind that our $w_p(r_p)$ measurements will be underestimated for $r_p < 0.3h^{-1}$Mpc, by roughly 20% on the smallest scales (see Coil et al. 2008).

4 RESULTS

4.1 Projected autocorrelation functions and bias factors

In Figure 1 we show projected stellar mass autocorrelation functions $w_p^*(r_p)$, as well as projected luminosity autocorrelations $w_p^L(r_p)$ in the U, B, V bands. Results are plotted for the SDSS in the left-hand panel, for the DEEP2 in the right-hand panel. In both panels $w_p^*(r_p)$ is shown using triangles with error bars, while the $w_p^L(r_p)$ are shown using lines.

The left-hand panel of Figure 1 reproduces the results of Paper II where luminosity autocorrelation functions were estimated for the five passbands of SDSS (*ugriz*). Luminosity is less strongly clustered than stellar mass on all scales and in all wavebands. Furthermore, the amplitude and slope of the luminosity autocorrelation function changes systematically with wavelength, with the reddest band (the V-band) showing the highest amplitude and the steepest slope. As a result, V-band light clusters more similarly to stellar mass than the bluer bands plotted, but not as closely as the z-band light analysed in Paper II. This is expected because z-band light is known to be closely related to stellar mass indicators (e.g. Kauffmann et al. 2003). Finally, all the autocorrelation estimates are well described by power laws. The best power-law fit to the stellar mass autocorrelations is shown in the figure, but in this paper we will not discuss such fits further, since they were a major topic of the two previous papers and the DEEP2 data do not allow autocorrelation shapes to be studied in as much detail as is possible at low redshift using SDSS.

As can be seen from the right-hand panel of Figure 1, the DEEP2 galaxies show very similar autocorrelation behaviour to the SDSS. Although the measurement errors are relatively large due to the smaller sample size and the considerable depth of the DEEP2, all the systematic trends seen above for the SDSS hold also for the DEEP2. Furthermore, the slopes of the autocorrelation functions are consistent with remaining constant from $z \sim 1$ to the present, although their amplitudes have increased by a factor of about 2 when, as here, they are measured in comoving coordinates. This is broadly consistent with previous studies of the evolution of galaxy two-point correlation functions using data from the same surveys (e.g. Coil et al. 2006, 2008).

These results are shown again in Figure 2 in terms of *bias factors* which we define as the ratio of the projected stellar mass (or luminosity) autocorrelation to the projected dark matter density autocorrelation. The latter is obtained from the $z = 0.065$ and $z = 1$ snapshots of the Millennium Simulation and thus assumes the cosmological parameters of the simulation. As noted above, these

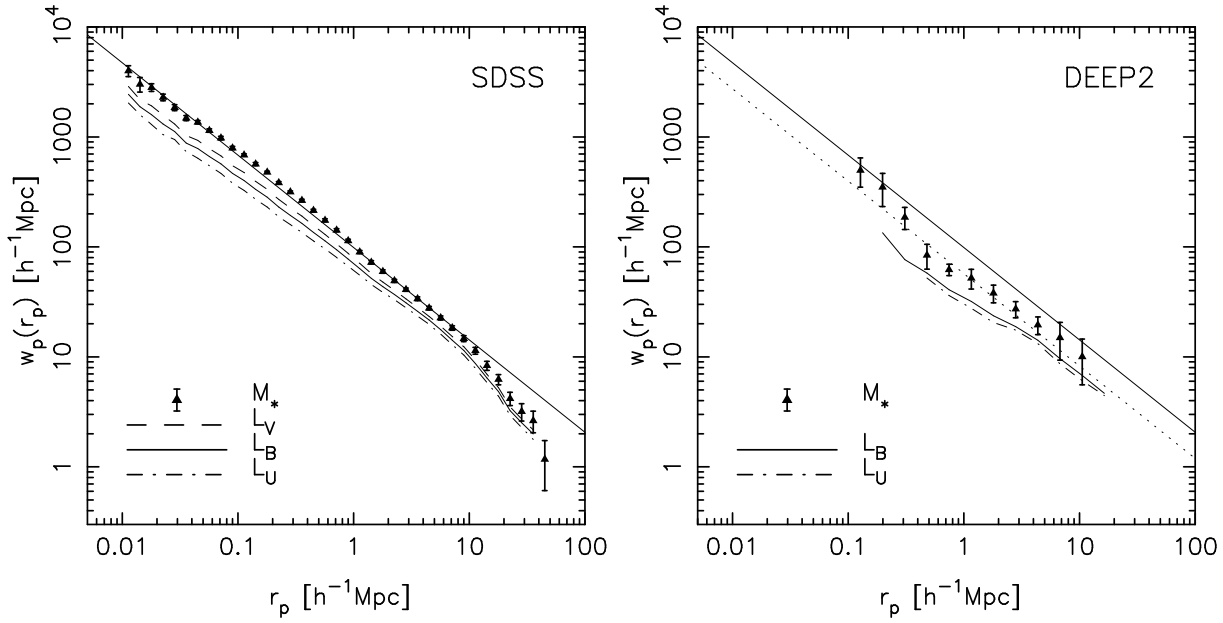

Figure 1. Projected stellar mass autocorrelation functions in the SDSS/DR7 (left panel) and in the DEEP2/DR3 (right panel) are plotted as triangles with error bars and are compared to projected luminosity autocorrelation functions measured in the rest-frame U, B and V bands (lines). Errors on the stellar mass autocorrelation function are estimated in the left panel from the scatter among measurements on 20 mock SDSS catalogues constructed from the Millennium Simulation, and in the right panel from the scatter between measurements on the four independent fields of the DEEP2 survey. The solid line in the left panel is a power-law fit to the SDSS data over the range $10h^{-1}kpc < r_p < 10h^{-1}Mpc$ and is repeated in the right panel. It corresponds to a three-dimensional autocorrelation function $\xi^*(r) = (r/r_0)^{-1.84}$ with $r_0 = 6.1h^{-1}Mpc$. The dotted line in the right panel is a power-law fit to the DEEP2 data over the full range probed, with index fixed to be -1.84, i.e. the same as what is determined for the SDSS data. The corresponding correlation length is $r_0 = 4.3h^{-1}Mpc$.

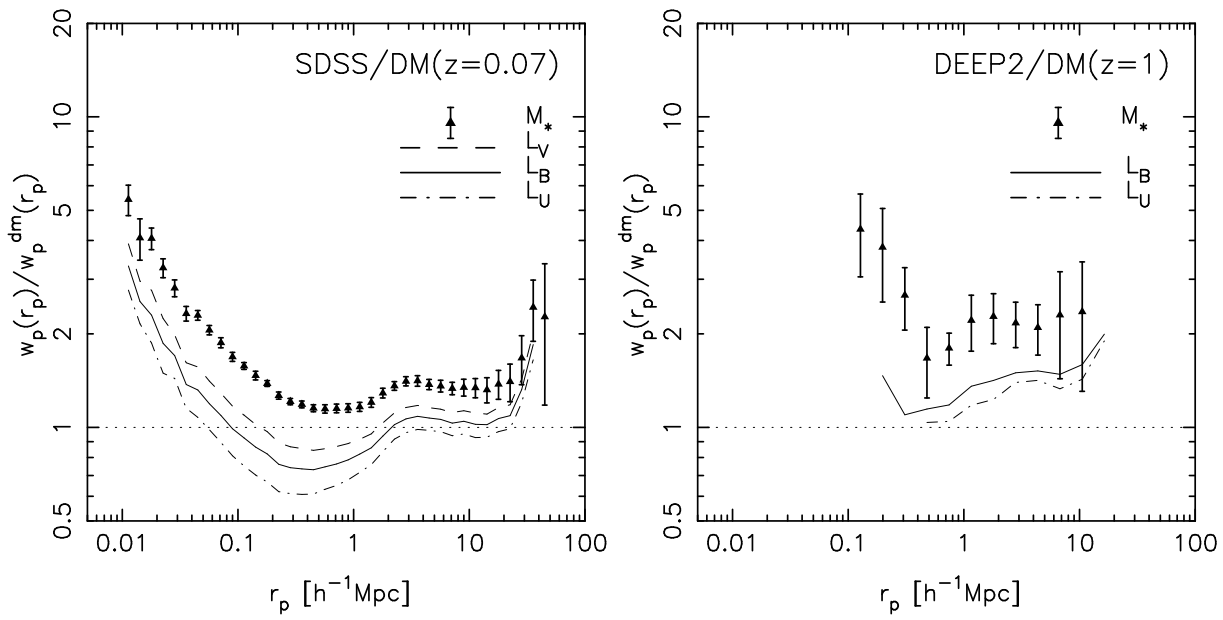

Figure 2. Ratio of the projected stellar mass (triangles) and luminosity (lines) autocorrelation functions in the SDSS/DR7 (left panel) and in the DEEP2/DR3 (right panel) to the projected dark matter autocorrelation function at $z = 0.07$ (left panel) and at $z = 1$ (right panel) in the Millennium Simulation. Errors on the stellar mass autocorrelations are estimated as in Fig. 1. Errors on the simulated functions are much smaller.

redshifts are appropriate to characterise the mean depth of our SDSS and DEEP2 measurements. A maximum line-of-sight depth $|\Delta\pi| = 40h^{-1}$Mpc was adopted when computing the projected autocorrelation function for dark matter in order to mimic our procedures for the real data. At $r_p \gtrsim 1.5h^{-1}$Mpc all our estimates are consistent with bias being scale-independent. On these scales the overall bias at $z \sim 1$ is higher by a factor of ~ 1.5 than at $z \sim 0$. This reflects the well-established result that large-scale structure has been growing more rapidly in the dark matter distribution since $z = 1$ than in the galaxy distribution.

At smaller separations the scale-dependence of the bias is strong, with a total range of a factor of 5 over $10h^{-1}$kpc$< r_p < 1h^{-1}$Mpc in the SDSS, and a factor of 2 over $100h^{-1}$kpc$< r_p < 1h^{-1}$Mpc in the DEEP2. Another obvious feature is a *step* at around 2 Mpc which is seen in all bias functions and at both redshifts. Given the featureless $w_p(r_p)$ observed for stellar mass and light, the strong scale dependence of the bias factors on these scales is largely due to the much more pronounced features seen in the dark matter autocorrelations, mainly the remarkable change in slope at the transition between the one-halo term, where the pair counts are dominated by galaxy pairs in the same halo, and the two-halo term, where galaxy pairs are mostly in separate haloes, at a few Mpc (see figures 2 and 6 of Paper I for illustrations). As discussed in Paper I, this uncomfortable step feature suggests that the amplitude of mass fluctuations is too high in the Millennium Simulations, and that the shape of our bias functions might be used to estimate the value of the fluctuation amplitude parameter σ_8. We will come back to this point in the last section.

4.2 Comparisons with a galaxy formation model

In this section we compare the observed projected autocorrelations of stellar light and mass to predictions for these same statistics from the galaxy formation model of G11, based on the Millennium and Millennium-II simulations. In their paper these authors already compared their model to SDSS clustering data, in particular, to the projected autocorrelations of stellar mass and of galaxies separated into passive and actively star-forming objects in a series of disjoint ranges of total stellar mass. They found their model to reproduce observed clustering reasonably well, to a level better than about 20% at all separations for $M_* \geqslant 6\times10^{10}M_\odot$ and at $r_p > 2$ Mpc for $M_* > 6\times10^{9}M_\odot$, but to substantially overpredict the clustering of stellar mass at smaller separations. Further comparisons between the SDSS and the model for autocorrelation functions in different intervals of stellar mass and optical colour showed this discrepancy to be due mainly to passive galaxies with stellar masses in the range $6\times10^{9}M_\odot < M_* < 6\times10^{10}M_\odot$, indicating that the model predicts too many red, passive, satellites of this mass [3]. The authors suggested that this might indicate that the fluctuation amplitude $\sigma_8 = 0.9$ adopted in the simulations is too high.

Here we extend this study to $z = 1$ by comparing the model predictions with our DEEP2 results. The results are shown in Figure 3 (the right-hand panel), where we plot the ratios of observed to predicted $w_p(r_p)$ both for stellar mass (symbols with error bars) and for luminosity in the U, B and V bands (lines). For comparison, the corresponding results for SDSS are shown in the left-hand panel. At both redshifts the discrepancy between model and data is clearest in the stellar mass autocorrelations. As already found by Guo et al. (2011), the model $w_p^*(r_p)$ exceeds that observed in the SDSS on all scales, by only $\sim$15% for $r_p \gtrsim 2h^{-1}$Mpc but by increasingly larger factors on smaller scales, reaching a factor of ~ 3 at $10h^{-1}$kpc. At a redshift $z \sim 1$ our DEEP2 results show a similar offset and are consistent with the same trend within their error bars.

Remarkably, although the model predicts stellar mass autocorrelations that disagree with the SDSS data, its luminosity autocorrelations match observation much better, particularly in the rest-frame B-band. Apparently the overly strong clustering of stellar mass is almost exactly compensated by the overabundance of passive satellite galaxies so that the light distribution is well reproduced. At $z \sim 1$ the predicted luminosity autocorrelations lie somewhat above the DEEP2 measurements in B but agree well at U. Given the error bars, the discrepancy at the longer wavelengths is only marginally significant. The fact that a physically based galaxy formation model can simultaneously agree with the clustering of light and disagree with that of stellar mass, yet agree with the abundance of galaxies as a function of both light and stellar mass (see G11) demonstrates the complexity of the constraints on galaxy formation implied by precise observations of abundance and clustering. The agreements and disagreements with DEEP2 data at $z \sim 1$ are very similar to those with SDSS data at low redshift, suggesting that the model is treating the evolution and clustering of the galaxy population in a realistic way.

5 SUMMARY AND DISCUSSION

In this work we have estimated projected autocorrelation functions $w_p(r_p)$ for the stellar mass of galaxies and for their light in the U, B and V bands, using data both from the third data release of the DEEP2 Galaxy Redshift Survey and the final data release of the Sloan Digital Sky Survey (SDSS). We have compared these to projected autocorrelations of dark matter estimated from the Millennium Simulations at $z = 1$ and 0.07, the median redshifts of our galaxy samples, in order to investigate the bias of the clustering of stellar mass and light.

The dependence of clustering on luminosity and colour for galaxies in the DEEP2 was previously studied by Coil et al. (2006) and Coil et al. (2008): the former investigates the luminosity-dependence of galaxy clustering, while the latter investigates the joint color and luminosity-dependence. These studies show that the dependence of clustering on color is stronger than on luminosity. These findings are qualitatively very similar to those seen at low redshift in SDSS data (e.g. Zehavi et al. 2005; Li et al. 2006a; Zehavi et al. 2010). Their conclusion was that the correlations between environment and galaxy properties which are well known at $z = 0$ were, in fact, largely in place at $z = 1$. In this paper we have investigated these issues further by

[3] The "excess" of passive red satellite is well documented in the literature and seems to be a "common" problem for all recent galaxy formation models.

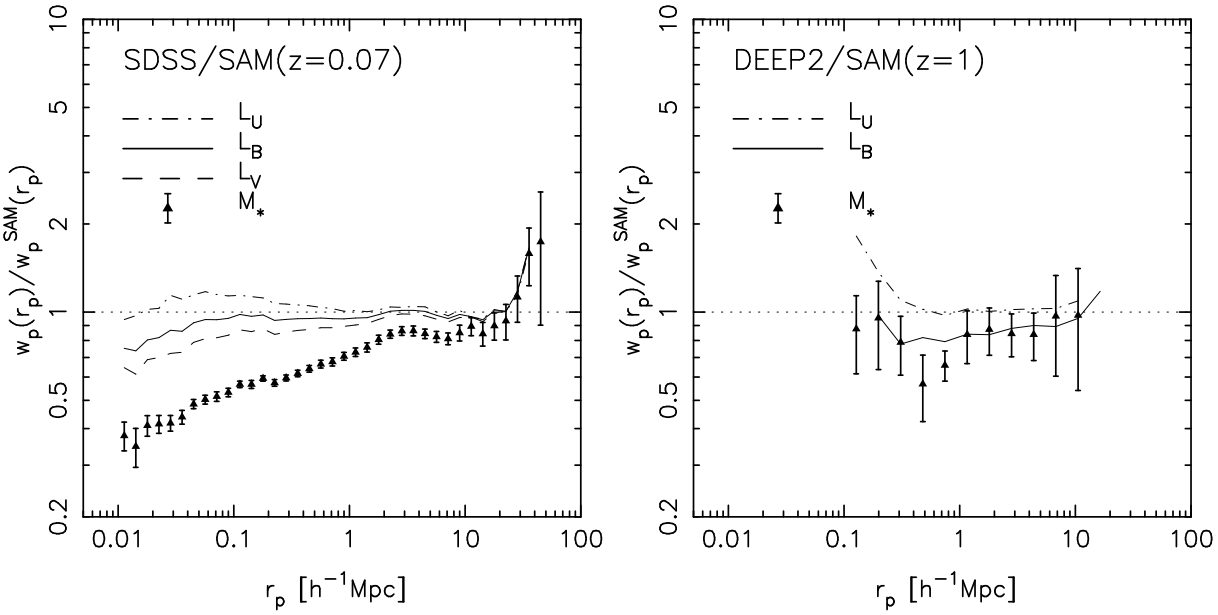

Figure 3. Ratio of the projected stellar mass (triangles) and luminosity (lines) autocorrelation functions in the SDSS/DR7 (left panel) and in the DEEP2/DR3 (right panel) to predictions of these same quantities from the semi-analytic galaxy formation simulation (SAM) of Guo et al. (2011) at $z = 0.07$ (left panel) and at $z = 1$ (right panel).

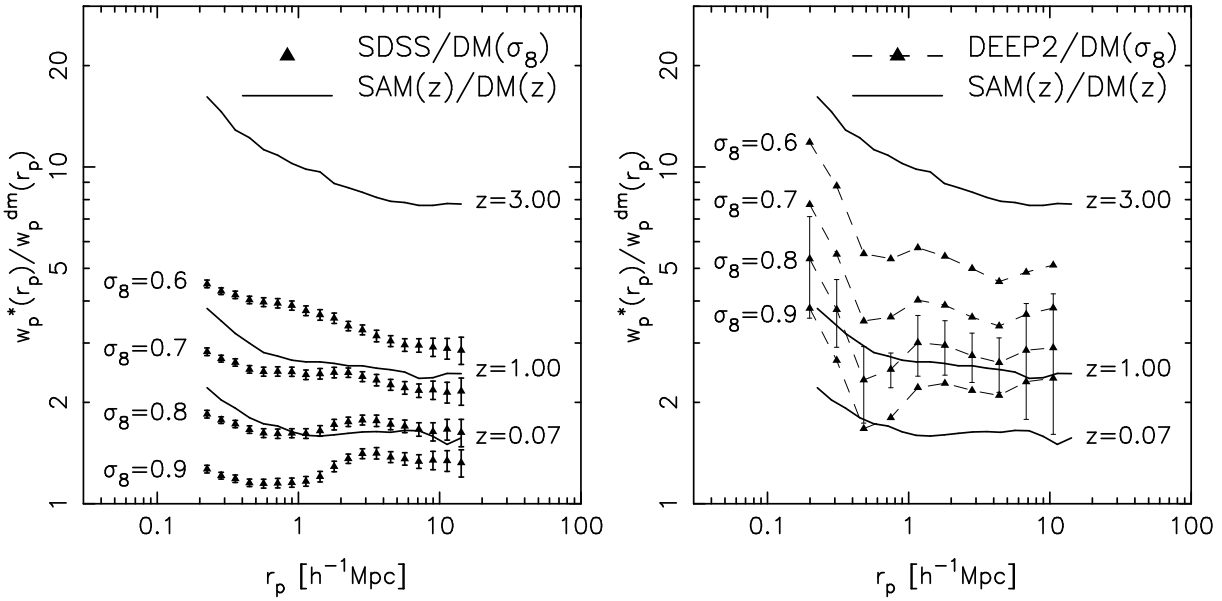

Figure 4. Triangles with error bars indicate bias as a function of scale for stellar mass in the SDSS (left panel) and in the DEEP2 (right panel) assuming the Millennium Simulation cosmology but with varying values (as labelled) for the present-day fluctuation amplitude σ_8. For σ_8 values other than 0.9, projected dark matter autocorrelations at $z = 0.07$ (for the SDSS) and $z = 1$ (for the DEEP2) are approximated by the functions found in the Millennium Simulation at earlier times when the linear fluctuation amplitude matches that desired. Bias functions for stellar mass in the Guo et al. (2011) galaxy formation model (which assumes $\sigma_8 = 0.9$) at $z = 0.07$, 1 and 3 are shown by solid lines, labelled by redshift. For clarity, error bars are only shown in the right-hand panel in the case $\sigma_8 = 0.8$, and the triangles for each σ_8 are connected by a dotted line. Only for $\sigma_8 = 0.8$ or 0.7 is the bias function inferred from the data approximately as flat and featureless at the one-halo/two-halo transition as that measured in the model.

evaluating alternative two-point statistics, the projected autocorrelations of stellar mass and light, in a uniform way for the SDSS and the DEEP2, so that the two surveys can be compared directly to each other and to the predictions of a recent MS-based simulation of the formation and evolution of the galaxy population (Guo et al. 2011). These statistics have some advantages in that they allow the full observed samples to be used to characterize the distribution of stars at high precision over the comoving ranges 10 kpc to 30 Mpc in the SDSS, and 200 kpc to 10 Mpc in DEEP2.

The most impressive result of this work is the remarkable similarity in behaviour between the SDSS and the DEEP2. The stellar mass and stellar light autocorrelations are, to within the still considerable error bars for DEEP2, identical in the two surveys except for an overall offset in amplitude by about a factor of two. Papers I and II have found that the autocorrelations of stellar mass (or luminosity) are dominated by contributions from galaxies in a relatively narrow range in mass (or luminosity), around the characteristic value of the stellar mass (or luminosity) function. In effect, this paper thus compares clustering of the population around M^* (or L^*) at the two redshifts. The similarity between the two surveys supports the conclusion of earlier analyses that the environmental dependence of galaxy properties seen in the local Universe was already in place at $z = 1$ (e.g. Coil et al. 2006, 2008; Cooper et al. 2006; Meneux et al. 2006, 2008, 2009). This similarity, as well as the factor-of-two offset between the two redshifts, are well reproduced by the galaxy formation model of G11 which matches the clustering of stellar light very well and overpredicts the clustering of stellar mass to a similar extent at both epochs.

The galaxy formation simulation fits the observed luminosity autocorrelations to within 30% on all scales, both at $z = 0$ and $z = 1$, and it fits the stellar mass autocorrelations to about 15% at $r_p > 2$ Mpc. On smaller scales the discrepancy in the stellar mass autocorrelations reaches a factor of 2 to 3. Correlations on large scales are produced by galaxies in different haloes (predominantly the central galaxies of those haloes) and the tight correlation between central galaxy properties and halo mass means that any model which fits the observed abundance of galaxies produces approximately correct correlations on these scales (e.g. Vale & Ostriker 2004; Conroy et al. 2006; Wang et al. 2006; More et al. 2009; Moster et al. 2010; Guo et al. 2010). Smaller scale correlations result from galaxy pairs residing in the same halo, so the discrepancy on these scales shows that the model has too many pairs of relatively massive galaxies which share a common halo. This may be explained by too large a value of σ_8 in the Millennium Simulations, which results in too many high-mass haloes which would then host these pairs. The much better agreement of the stellar light autocorrelations on these same scales, shows that the "extra" satellite galaxies must have relatively little light for their mass, thus high stellar mass-to-light ratios.

An interesting feature in the observed bias functions of Fig. 2 is the obvious step at the one-halo/two-halo transition at about 2 Mpc which reflects the marked change in slope of the dark matter correlations at this point (see figs. 2 and 6 of Paper I). We noted in Paper I that since physically consistent models for the evolution of the dark matter and galaxy distributions show smooth bias behaviour over this separation range, this feature suggests that the amplitude of mass fluctuations is too high in the Millennium Simulation, producing a one-halo/two-halo transition which is stronger in the simulated mass distribution than in the true mass distribution. If this interpretation is correct, the shape of our bias functions can be used to estimate the value of the fluctuation amplitude parameter σ_8. We illustrate this possibility in Figure 4 where we plot the bias determined from the clustering of stellar mass over the separation range $200h^{-1}kpc < r_p < 15h^{-1}Mpc$ both for the SDSS ($z = 0.07$) and for the DEEP2 ($z = 1$). Here we use dark matter correlations measured in the Millennium Simulation not only at the median redshifts of the observed samples, but also at higher redshifts in order to represent (approximately) the correlations expected at the observed redshifts in cosmologies similar to the Millennium cosmology but with lower σ_8. We choose earlier redshifts with linear fluctuation amplitudes corresponding to $\sigma_8 = 0.8$, 0.7 and 0.6. The filled triangles show estimates of the stellar mass bias for the two surveys made in this way for four different values of σ_8. It is clear that as the fluctuation amplitude is decreased the step feature becomes less prominent in both surveys and the bias becomes a more strongly decreasing function of scale.

Theoretical predictions for these stellar mass bias functions for $z = 0.07$, 1 and 3 are shown for the galaxy formation model of G11 as solid lines in Figure 4. As for the earlier galaxy formation models plotted in Paper I, none of these curves shows a feature at the one-halo/two-halo transition, but their slope increases significantly towards higher redshift. Comparing with the observational results, it is clear that the the best agreement in amplitude occurs for $\sigma_8 = 0.8$ whereas the overall shape agrees best for somewhat lower amplitudes. It is remarkable that these results hold both for the SDSS at $z = 0.07$ and for the DEEP2 at $z = 1$. Hence the models appear to describe the overall evolution of the stellar mass autocorrelations surprisingly well, once the cosmology is corrected to a lower σ_8 value, similar to that indicated by most other recent analyses of CMB and other data (e.g. Komatsu et al. 2009, 2010).

ACKNOWLEDGMENTS

CL is supported by the Bairen Program of the Chinese Academy of Sciences (CAS) and the exchange program between the Max Planck Society and the CAS. CL and YPJ are supported by NSFC (no. 10533030), by 973 Program (no. 2007CB815402) and by the Knowledge Innovation Program of CAS (no. KJCX2-YW-T05). GDL acknowledges financial support from the European Research Council under the European Community's Seventh Framework Programme (FP7/2007- 2013)/ERC grant agreement n. 202781. WZ acknowledges financial support from NSFC (no. 10903011).

Funding for the DEEP2 Galaxy Redshift Survey has been provided in part by NSF grant AST00-71048 and NASA LTSA grant NNG04GC89G.

Funding for the SDSS and SDSS-II has been provided by the Alfred P. Sloan Foundation, the Participating Institutions, the National Science Foundation, the U.S. Department of Energy, the National Aeronautics and Space Administration, the Japanese Monbukagakusho, the Max Planck Society, and the Higher Education Funding Council for England. The SDSS Web Site is http://www.sdss.org/. The SDSS is managed by the Astrophysical Research Consortium for the Participating Institutions. The Participating Institutions are the American Museum of Natural History, Astrophysical Institute Potsdam, University of Basel, University of Cambridge, Case Western Reserve University, University of Chicago, Drexel University, Fermilab, the Institute for Advanced Study, the Japan Participation Group, Johns Hopkins University, the Joint Institute for Nuclear Astrophysics, the Kavli Institute for Particle As-

trophysics and Cosmology, the Korean Scientist Group, the Chinese Academy of Sciences (LAMOST), Los Alamos National Laboratory, the Max-Planck-Institute for Astronomy (MPIA), the Max-Planck-Institute for Astrophysics (MPA), New Mexico State University, Ohio State University, University of Pittsburgh, University of Portsmouth, Princeton University, the United States Naval Observatory, and the University of Washington.

REFERENCES

Abazajian K. N., Adelman-McCarthy J. K., Agüeros M. A., Allam S. S., Allende Prieto C., An D., Anderson K. S. J., Anderson S. F., et al., 2009, ApJS, 182, 543
Beisbart C., Kerscher M., 2000, ApJ, 545, 6
Benoist C., Maurogordato S., da Costa L. N., Cappi A., Schaeffer R., 1996, ApJ, 472, 452
Boerner G., Mo H., Zhou Y., 1989, A&A, 221, 191
Boylan-Kolchin M., Springel V., White S. D. M., Jenkins A., Lemson G., 2009, MNRAS, 398, 1150
Brown M. J. I., Webster R. L., Boyle B. J., 2000, MNRAS, 317, 782
Bruzual G., Charlot S., 2003, MNRAS, 344, 1000
Bundy K., Ellis R. S., Conselice C. J., Taylor J. E., Cooper M. C., Willmer C. N. A., Weiner B. J., Coil A. L., et al., 2006, ApJ, 651, 120
Coil A. L., Davis M., Madgwick D. S., Newman J. A., Conselice C. J., Cooper M., Ellis R. S., Faber S. M., et al., 2004a, ApJ, 609, 525
Coil A. L., Newman J. A., Cooper M. C., Davis M., Faber S. M., Koo D. C., Willmer C. N. A., 2006, ApJ, 644, 671
Coil A. L., Newman J. A., Croton D., Cooper M. C., Davis M., Faber S. M., Gerke B. F., Koo D. C., et al., 2008, ApJ, 672, 153
Coil A. L., Newman J. A., Kaiser N., Davis M., Ma C.-P., Kocevski D. D., Koo D. C., 2004b, ApJ, 617, 765
Colless M., Dalton G., Maddox S., Sutherland W., Norberg P., Cole S., Bland-Hawthorn J., Bridges T., et al., 2001, MNRAS, 328, 1039
Conroy C., Wechsler R. H., Kravtsov A. V., 2006, ApJ, 647, 201
Cooper M. C., Newman J. A., Croton D. J., Weiner B. J., Willmer C. N. A., Gerke B. F., Madgwick D. S., Faber S. M., et al., 2006, MNRAS, 370, 198
Davis M., Faber S. M., Newman J., Phillips A. C., Ellis R. S., Steidel C. C., Conselice C., Coil A. L., et al., 2003, in Society of Photo-Optical Instrumentation Engineers (SPIE) Conference Series, Guhathakurta P., ed., Vol. 4834, pp. 161–172
Davis M., Meiksin A., Strauss M. A., da Costa L. N., Yahil A., 1988, ApJ, 333, L9
de la Torre S., Le Fèvre O., Porciani C., Guzzo L., Meneux B., Abbas U., Tasca L., Carollo C. M., et al., 2011a, MNRAS, 412, 825
de la Torre S., Meneux B., De Lucia G., Blaizot J., Le Fèvre O., Garilli B., Cucciati O., Mellier Y., et al., 2011b, A&A, 525, A125+
De Lucia G., Blaizot J., 2007, MNRAS, 375, 2
Einasto M., 1991, MNRAS, 252, 261
Faber S. M., Phillips A. C., Kibrick R. I., Alcott B., Allen S. L., Burrous J., Cantrall T., Clarke D., et al., 2003, in Society of Photo-Optical Instrumentation Engineers (SPIE) Conference Series, Moorwood M. I. . A. F. M., ed., Vol. 4841, pp. 1657–1669
Faltenbacher A., Gottlöber S., Kerscher M., Müller V., 2002, A&A, 395, 1
Guo Q., White S., Boylan-Kolchin M., De Lucia G., Kauffmann G., Lemson G., Li C., Springel V., et al., 2011, MNRAS, 413, 101
Guo Q., White S., Li C., Boylan-Kolchin M., 2010, MNRAS, 404, 1111
Guzzo L., Bartlett J. G., Cappi A., Maurogordato S., Zucca E., Zamorani G., Balkowski C., Blanchard A., et al., 2000, A&A, 355, 1
Guzzo L., Strauss M. A., Fisher K. B., Giovanelli R., Haynes M. P., 1997, ApJ, 489, 37
Hamilton A. J. S., 1988, ApJ, 331, L59
Kauffmann G., Heckman T. M., White S. D. M., Charlot S., Tremonti C., Brinchmann J., Bruzual G., Peng E. W., et al., 2003, MNRAS, 341, 33
Komatsu E., Dunkley J., Nolta M. R., Bennett C. L., Gold B., Hinshaw G., Jarosik N., Larson D., et al., 2009, ApJS, 180, 330
Komatsu E., Smith K. M., Dunkley J., Bennett C. L., Gold B., Hinshaw G., Jarosik N., Larson D., et al., 2010, ArXiv e-prints
Kroupa P., 2001, MNRAS, 322, 231
Le Fèvre O., Guzzo L., Meneux B., Pollo A., Cappi A., Colombi S., Iovino A., Marinoni C., et al., 2005, A&A, 439, 877
Li C., Jing Y. P., Kauffmann G., Börner G., Kang X., Wang L., 2007, MNRAS, 376, 984
Li C., Jing Y. P., Kauffmann G., Börner G., White S. D. M., Cheng F. Z., 2006a, MNRAS, 368, 37
Li C., Kauffmann G., Jing Y. P., White S. D. M., Börner G., Cheng F. Z., 2006b, MNRAS, 368, 21
Li C., White S. D. M., 2009, MNRAS, 398, 2177
—, 2010, MNRAS, 407, 515
Lilly S. J., Le Brun V., Maier C., Mainieri V., Mignoli M., Scodeggio M., Zamorani G., Carollo M., et al., 2009, ApJS, 184, 218
Lilly S. J., Le Fèvre O., Renzini A., Zamorani G., Scodeggio M., Contini T., Carollo C. M., Hasinger G., et al., 2007, ApJS, 172, 70
Loveday J., Maddox S. J., Efstathiou G., Peterson B. A., 1995, ApJ, 442, 457
Loveday J., Tresse L., Maddox S., 1999, MNRAS, 310, 281
Meneux B., Guzzo L., de la Torre S., Porciani C., Zamorani G., Abbas U., Bolzonella M., Garilli B., et al., 2009, A&A, 505, 463
Meneux B., Guzzo L., Garilli B., Le Fèvre O., Pollo A., Blaizot J., De Lucia G., Bolzonella M., et al., 2008, A&A, 478, 299
Meneux B., Le Fèvre O., Guzzo L., Pollo A., Cappi A., Ilbert O., Iovino A., Marinoni C., et al., 2006, A&A, 452, 387
More S., van den Bosch F. C., Cacciato M., Mo H. J., Yang X., Li R., 2009, MNRAS, 392, 801
Moster B. P., Somerville R. S., Maulbetsch C., van den Bosch F. C., Macciò A. V., Naab T., Oser L., 2010, ApJ, 710, 903
Norberg P., Baugh C. M., Hawkins E., Maddox S., Madgwick D., Lahav O., Cole S., Frenk C. S., et al., 2002, MN-

RAS, 332, 827
Norberg P., Baugh C. M., Hawkins E., Maddox S., Peacock J. A., Cole S., Frenk C. S., Bland-Hawthorn J., et al., 2001, MNRAS, 328, 64
Park C., Vogeley M. S., Geller M. J., Huchra J. P., 1994, ApJ, 431, 569
Pollo A., Guzzo L., Le Fèvre O., Meneux B., Cappi A., Franzetti P., Iovino A., McCracken H. J., et al., 2006, A&A, 451, 409
Pollo A., Meneux B., Guzzo L., Le Fèvre O., Blaizot J., Cappi A., Iovino A., Marinoni C., et al., 2005, A&A, 439, 887
Ross A. J., Tojeiro R., Percival W. J., 2011, MNRAS, 413, 2078
Salim S., Charlot S., Rich R. M., Kauffmann G., Heckman T. M., Barlow T. A., Bianchi L., Byun Y.-I., et al., 2005, ApJ, 619, L39
Sheth R. K., 2005, MNRAS, 364, 796
Skibba R., Sheth R. K., Connolly A. J., Scranton R., 2006, MNRAS, 369, 68
Skibba R. A., Bamford S. P., Nichol R. C., Lintott C. J., Andreescu D., Edmondson E. M., Murray P., Raddick M. J., et al., 2009, MNRAS, 399, 966
Skibba R. A., Sheth R. K., 2009, MNRAS, 392, 1080
Springel V., 2005, MNRAS, 364, 1105
Swanson M. E. C., Tegmark M., Blanton M., Zehavi I., 2008, MNRAS, 385, 1635
Tegmark M., Blanton M. R., Strauss M. A., Hoyle F., Schlegel D., Scoccimarro R., Vogeley M. S., Weinberg D. H., et al., 2004, ApJ, 606, 702
Vale A., Ostriker J. P., 2004, MNRAS, 353, 189
Wang L., Li C., Kauffmann G., De Lucia G., 2006, MNRAS, 371, 537
Wang W., Jing Y. P., Li C., Okumura T., Han J., 2010, ArXiv e-prints
Wang Y., Yang X., Mo H. J., van den Bosch F. C., 2007, ApJ, 664, 608
White S. D. M., Tully R. B., Davis M., 1988, ApJ, 333, L45
Willmer C. N. A., da Costa L. N., Pellegrini P. S., 1998, AJ, 115, 869
Willmer C. N. A., Faber S. M., Koo D. C., Weiner B. J., Newman J. A., Coil A. L., Connolly A. J., Conroy C., et al., 2006, ApJ, 647, 853
Yan R., White M., Coil A. L., 2004, ApJ, 607, 739
York D. G., Adelman J., Anderson Jr. J. E., Anderson S. F., Annis J., Bahcall N. A., Bakken J. A., Barkhouser R., et al., 2000, AJ, 120, 1579
Zehavi I., Blanton M. R., Frieman J. A., Weinberg D. H., Mo H. J., Strauss M. A., Anderson S. F., Annis J., et al., 2002, ApJ, 571, 172
Zehavi I., Zheng Z., Weinberg D. H., Blanton M. R., Bahcall N. A., Berlind A. A., Brinkmann J., Frieman J. A., et al., 2010, ArXiv e-prints
Zehavi I., Zheng Z., Weinberg D. H., Frieman J. A., Berlind A. A., Blanton M. R., Scoccimarro R., Sheth R. K., et al., 2005, ApJ, 630, 1

This paper has been typeset from a TEX/ LATEX file prepared by the author.